

Supporting Information for

Set-up and screening of a fragment library targeting 14-3-3 protein interface

Dario Valenti,^{a,b†} João Filipe Neves,^{c†} François-Xavier Cantrelle,^c Stanimira Hristeva,^a Domenico Lentini Santo,^d Tomáš Obšil,^{d,e} Xavier Hanoulle,^c Laura M. Levy,^{a†} Dimitrios Tzalis,^{*a} Isabelle Landrieu^{*c†} and Christian Ottmann^{*b,f†}

^a. *Medicinal Chemistry, Taros Chemicals GmbH & Co. KG, Emil-Figge-Straße 76a, 44227, Dortmund, Germany. Email: dtzalis@taros.de*

^b. *Department of Biomedical Engineering and Institute for Complex Molecular Systems, Technische Universiteit Eindhoven, Den Dolech 2, 5612, AZ, Eindhoven, the Netherlands. Email: c.ottmann@tue.nl*

^c. *Univ. Lille, CNRS, UMR 8576 - UGSF - F-59000 Lille, France. Email: isabelle.landrieu@univ-lille.fr*

^d. *Department of Physical and Macromolecular Chemistry, Faculty of Science, Charles University, 12843 Prague, Czech Republic*

^e. *Department of Structural Biology of Signaling Proteins, Division BIOCEV, Institute of Physiology of the Czech Academy of Sciences, Prumyslova 595, 252 50 Vestec, Czech Republic*

^f.*Department of Chemistry, University of Duisburg-Essen, Universitätsstraße 7, 45117, Essen, Germany*

† Equal contribution.

Physico-chemical Filtering

Physico-chemical properties have been calculated by ChemAxon JChem for Excel (version 16.10.1700.1231).

Fragments' quality control and purification

The initial purity of each fragment was analysed by uHPLC-MS integrated systems. For each sample, 100 mg were weighted and dissolved in a mixture of Acetonitrile and Methanol in ratio 1:1. The non-soluble fragments were excluded from the collection. uHPLC-MS checks were performed using uHPLC Agilent Technologies 1290 Infinity coupled with Agilent Technologies 6120 Quadrupole LC/MS, Column: ACQUITY UPLC®BEH C18 1.7 µm, mobile phase: mixture of Acetonitrile + 0.1% Formic Acid and Water + 0.1% Formic Acid. When purity was below the 85% threshold, preparative HPLC was performed using UPLC Agilent Technologies 1260 Infinity coupled with Agilent Technologies 6120 Quadrupole LC/MS, Column: XBridge EH C18 5 µm, 19 mm x 150 mm, mobile phase: mixture of Acetonitrile + 0.1% Formic Acid and Water + 0.1% Formic Acid.

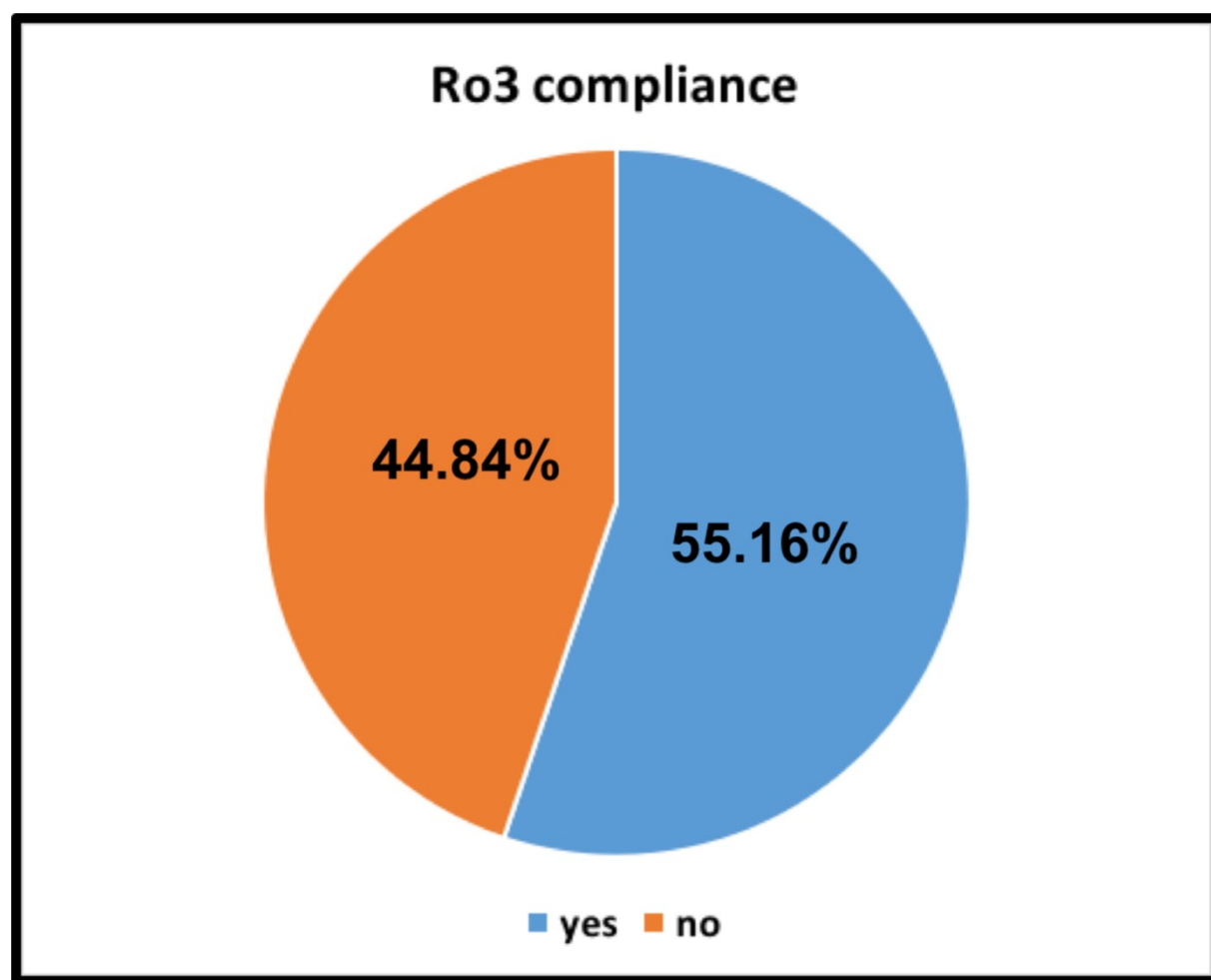


Chart S1. Ro3 compliance of the fragment collection.

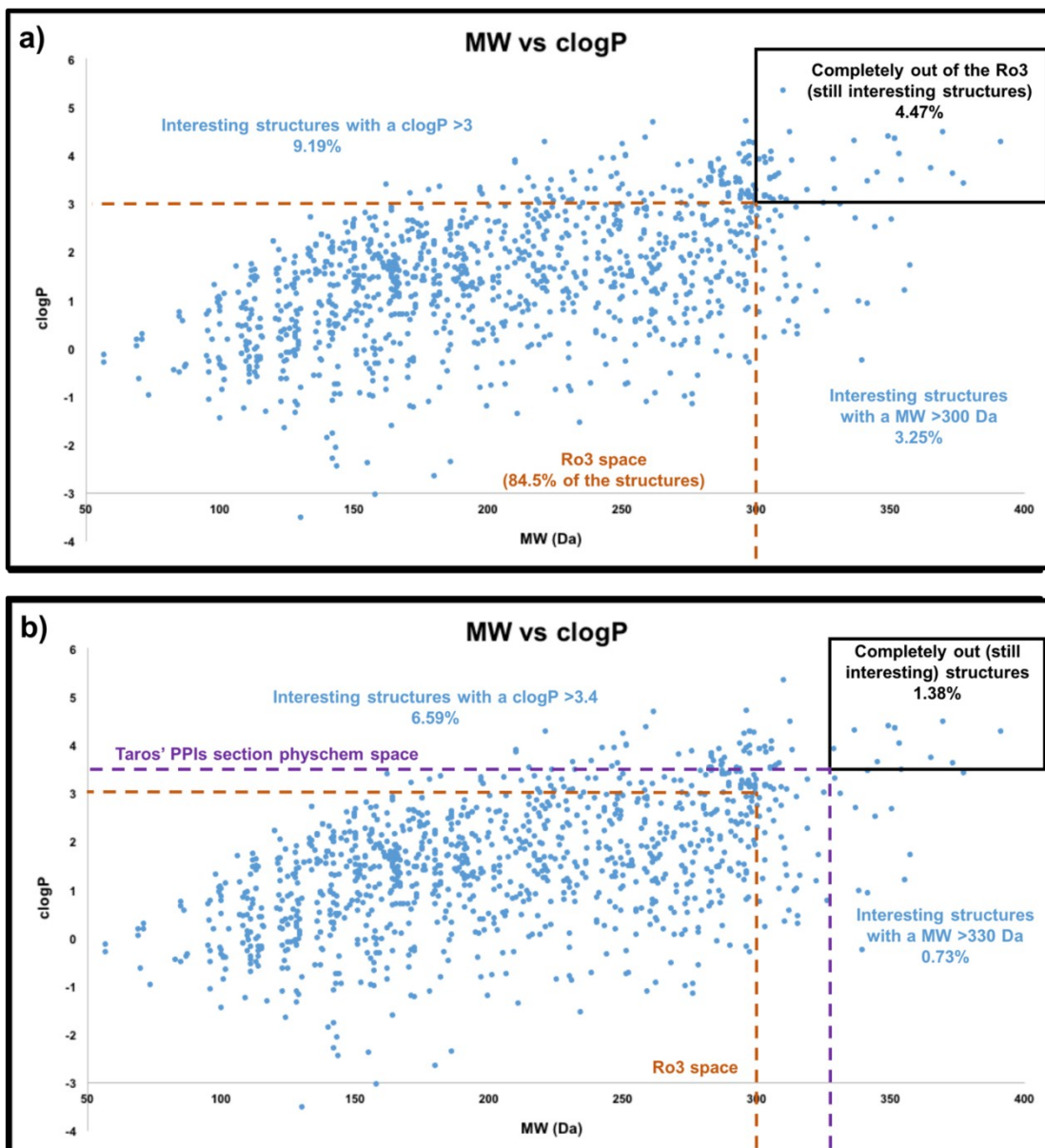


Figure S1. Fragments' MW and clogP distribution. Correlation between MW and clogP considering the classical Rule of Three parameters (A) or the revised limits (MW 330 Da and clogP 3.4) used for setting up the collection (B). Orange dashed line delimits the Rule of Three (Ro3) space that is included into the wider parameters selected for this particular subset of the Taros' fragment library (purple dashed lines, (B)) while the black box on the top right includes the entries with both MW and clogP out of the Ro3 space (A) or out of the Taros' PPIs physchem space (B). (A) 12% of the structures have at least one parameter out of the rule and only 4% of the entries have both MW and clogP outside of the rule but present promising structures. (B) The percentage of structures with MW or clogP parameters over the settings decrease to 7.3% (compared to (A)) while 1.4% present both MW and clogP over the set limits but nonetheless have attractive structures.

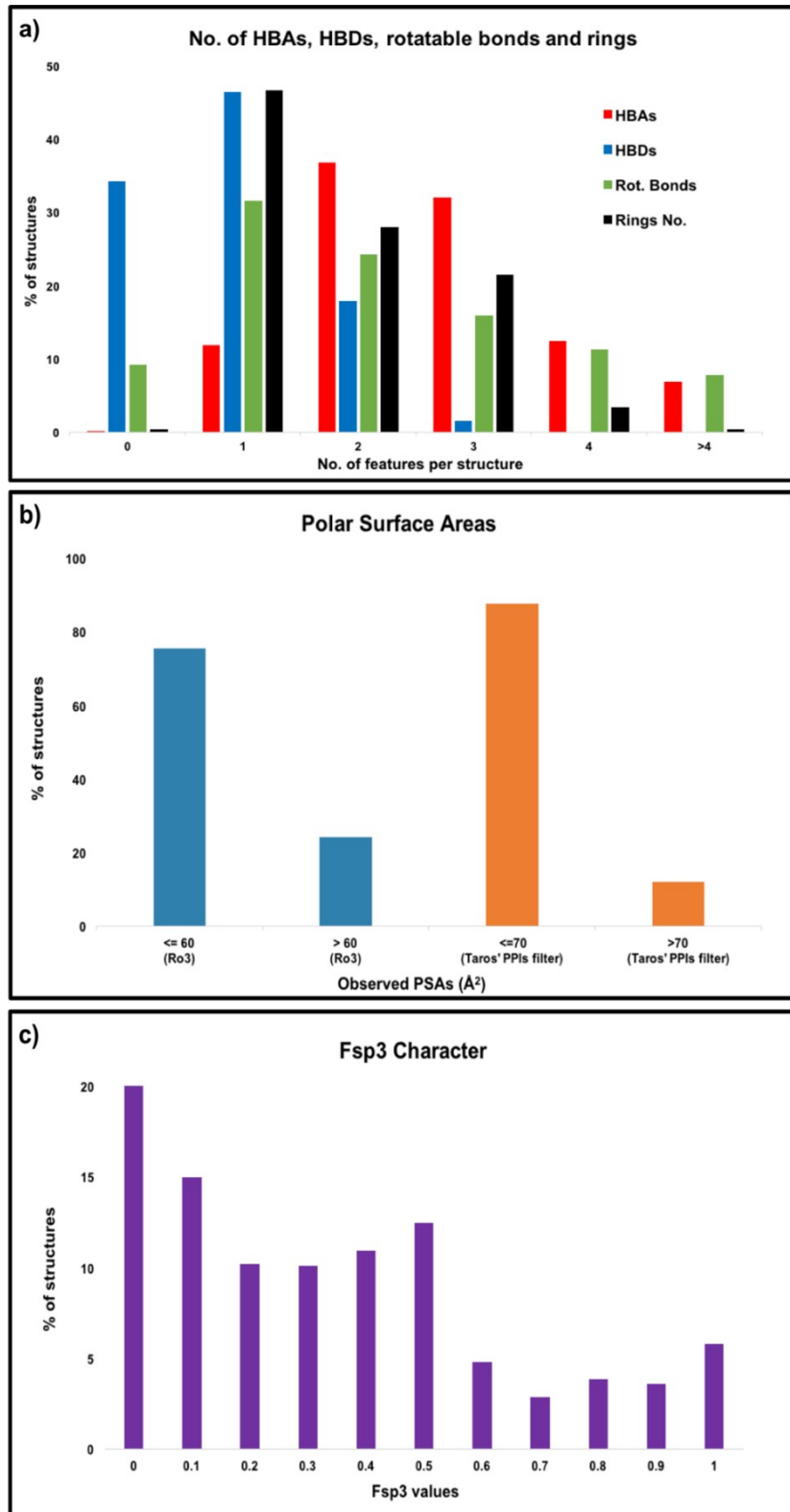


Figure S2. (A) Number of H-bond acceptors (HBAs), donors (HBDs), rotatable bonds (Rot. Bonds) and rings. The totality of the molecules presents no more than 3 HBDs while 80.7% has no more than 3 HBAs. Number of entries with no more than 3 rotatable bonds covers a similar percentage (80.9%). 96.4% of the structures contains no more than 3 rings. (B) Distribution of Polar Surface Areas, according to the Ro3 (cyan) and to the Taros' PPIs section parameters (orange). 75.7% has a PSA value below or equal the 60 \AA^2 threshold. According to our parameters ($\text{PSA} \leq 70 \text{ \AA}^2$) 87.9% of the molecules fit well the requirements. (C) Saturation character (Fsp3) distribution. More than half of the structures (55.8%) present a completely flat core while 28.2% have an intermediate saturation character and 16.1% of them show a fully three-dimensional character.

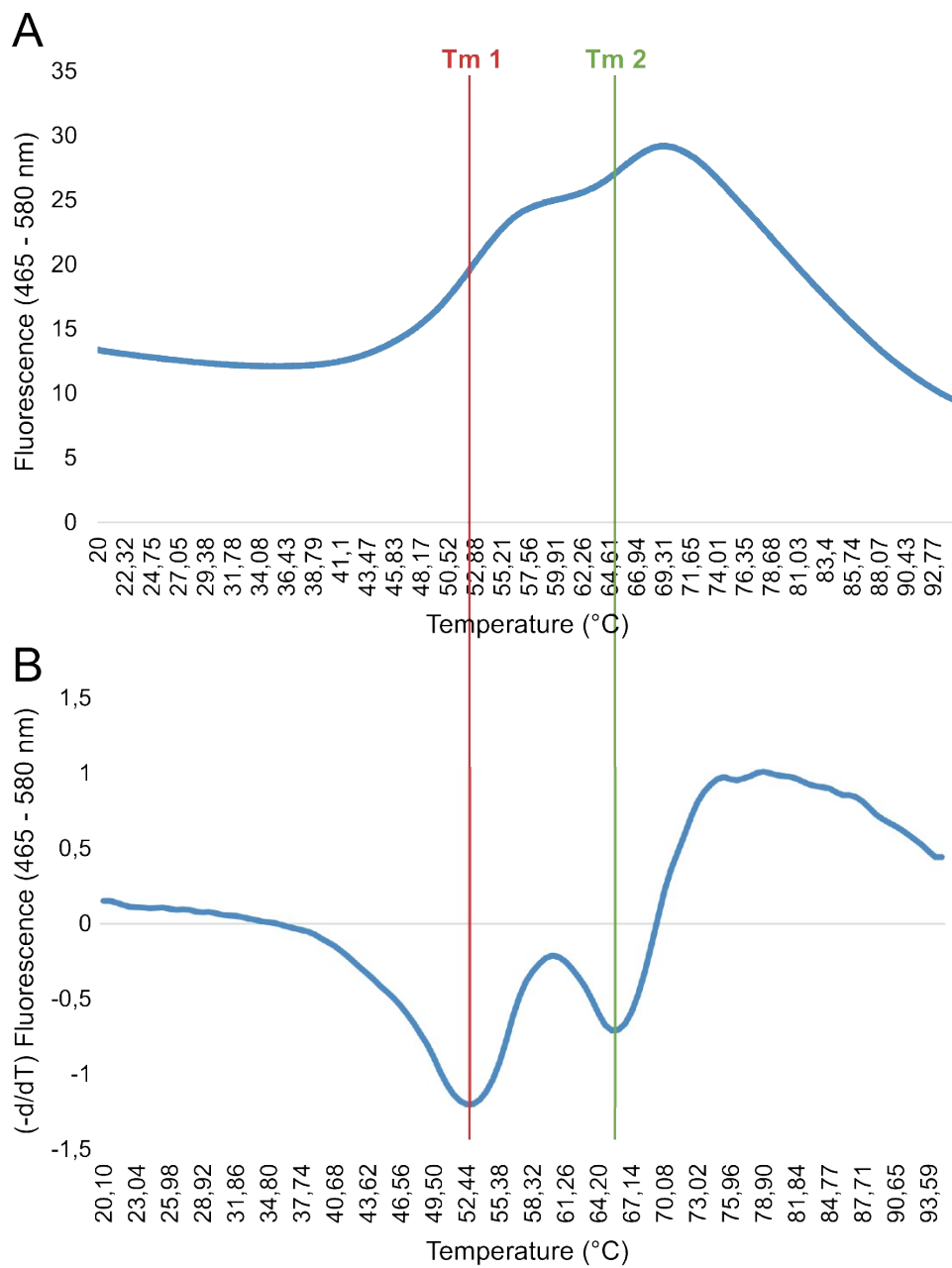


Figure S3. DSF analysis of melting temperatures of 14-3-3 σ in the presence of compounds. The melting curve of 14-3-3 σ 7 μ M in the presence of 4% DMSO is presented in A as the variation of fluorescence (y axis) as a function of the temperature (x axis). Two different melting temperatures, identified as Tm 1 (in red) and Tm 2 (in green) are observed in the melting curve of the protein. The first derivative of the melting curve is presented in B. The x axis represents the temperature, same scale as in A.

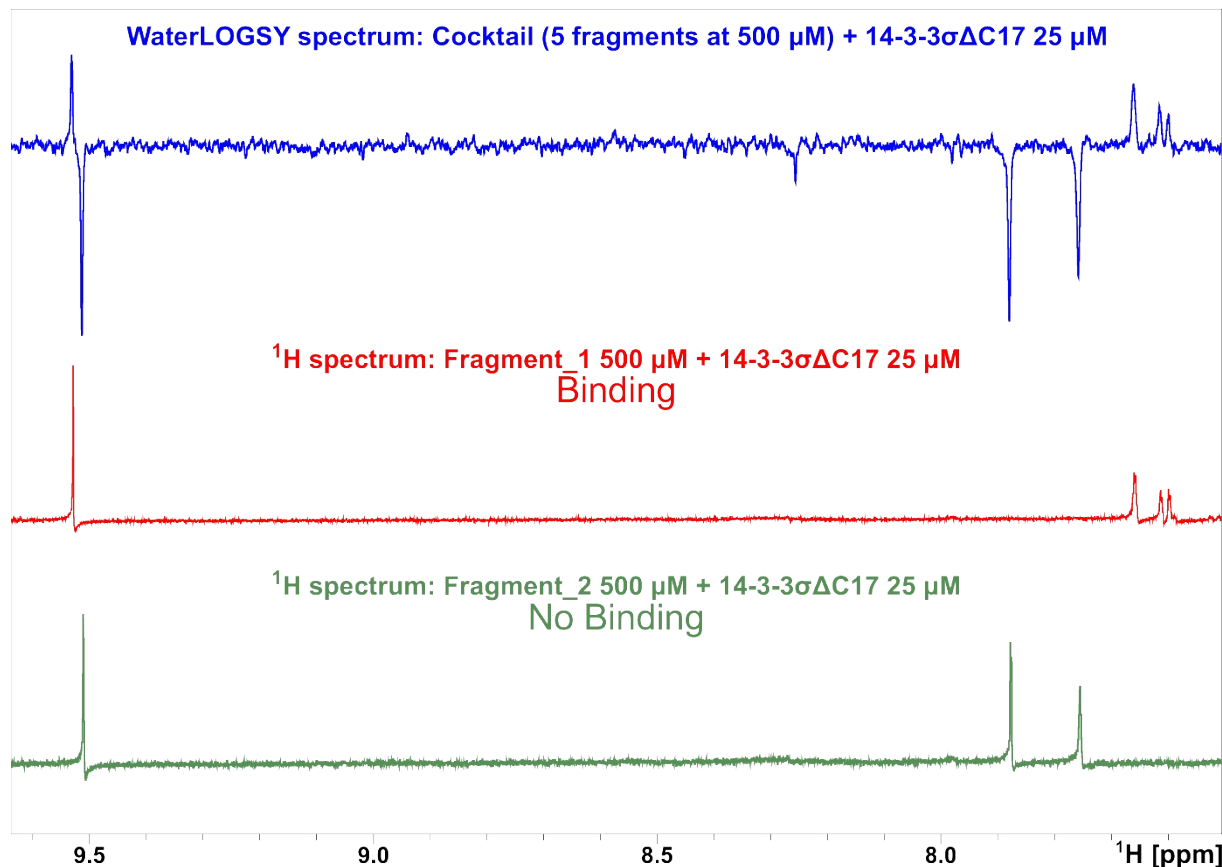


Figure S4. WaterLOGSY allows the determination of which singleton of the cocktail is binding to 14-3-3σΔC17. A WaterLOGSY spectrum of a Cocktail is shown at the top, in blue. A ¹H spectrum of a hit singleton (Fragment_1) of the same cocktail is presented below the WaterLOGSY spectrum, in red. Note that the resonances of this molecule are positive in the WaterLOGSY spectrum, showing that this molecule binds to 14-3-3σΔC17. At the bottom, a ¹H spectrum of a non-binder singleton (Fragment_2) is shown in green. Note that the resonances of this molecule are negative in the WaterLOGSY spectrum of the cocktail, meaning that this compound does not bind to 14-3-3σΔC17. The three spectra are referenced equally and were acquired in the same conditions.

Table S1. DSF melting temperature data for the screened cocktail library. The average melting temperatures, standard deviations and induced thermal shifts (ΔT_m) are reported for each cocktail.

COCKTAIL	Average Tm 1 (°C) n=3	SD Tm 1 (°C) n=3	ΔT_m 1 (°C)	Average Tm 2 (°C) n=3	SD Tm 2 (°C) n=3	ΔT_m 2 (°C)	ΔT_m 1 + ΔT_m 2 (°C)
1	52,54	0,11	-0,31	65,69	0,19	-0,03	0,35
2	53,02	0,06	0,16	66,33	0,06	0,60	0,76
3	52,92	0,15	0,06	66,35	0,25	0,63	0,69
4	52,80	0,11	-0,06	65,82	0,20	0,09	0,15
5	52,73	0,05	-0,13	65,76	0,06	0,03	0,16
6	52,89	0,15	0,03	66,04	0,20	0,31	0,35
7	52,98	0,06	0,13	66,20	0,27	0,47	0,60
8	52,57	0,10	-0,28	65,60	0,09	-0,13	0,41
9	52,54	0,05	-0,32	65,88	0,00	0,15	0,47
10	51,50	0,11	-1,35	66,07	0,10	0,35	1,70
11	-	-	-	-	-	-	-
12	51,57	0,11	-1,29	66,13	0,11	0,41	1,70
13	52,81	0,06	-0,05	65,79	0,17	0,06	0,11
14	52,76	0,10	-0,09	65,82	0,24	0,09	0,19
15	53,11	0,14	0,25	66,23	0,24	0,50	0,75
16	53,17	0,10	0,31	66,20	0,11	0,47	0,78
17	52,95	0,10	0,10	65,95	0,14	0,22	0,32
18	52,64	0,24	-0,22	65,69	0,16	-0,03	0,25
19	53,14	0,28	0,28	66,32	0,22	0,60	0,88
20	53,20	0,14	0,35	66,42	0,14	0,69	1,04
21	52,54	0,20	-0,32	65,73	0,11	0,00	0,32
22	52,98	0,38	0,13	66,20	0,05	0,47	0,60
23	52,95	0,10	0,10	66,13	0,11	0,41	0,50
24	53,11	0,20	0,25	66,39	0,11	0,66	0,91
25	52,67	0,19	-0,19	66,04	0,31	0,31	0,50
26	52,73	0,11	-0,12	66,20	0,11	0,47	0,59
27	53,11	0,20	0,25	66,48	0,05	0,75	1,01
28	53,05	0,10	0,19	66,23	0,24	0,50	0,69
29	52,86	0,00	0,00	66,17	0,00	0,44	0,45
30	53,02	0,14	0,16	66,26	0,17	0,54	0,70
31	52,73	0,20	0,19	66,07	0,10	-0,03	0,22
32	52,67	0,17	0,12	65,76	0,29	-0,35	0,47
33	52,54	0,33	0,00	66,13	0,29	0,03	0,03
34	52,58	0,43	0,03	66,04	0,24	-0,06	0,10
35	52,48	0,10	-0,07	66,04	0,20	-0,06	0,13
36	43,32	0,25	-9,22	65,09	0,11	-1,01	10,23
37	52,94	0,42	0,40	66,04	0,13	-0,06	0,46
38	52,51	0,11	-0,04	65,94	0,11	-0,16	0,20
39	52,32	0,28	-0,22	66,04	0,15	-0,06	0,29
40	52,79	0,45	0,25	65,88	0,10	-0,22	0,47

41	52,83	0,06	0,28	65,69	0,16	-0,41	0,69
42	52,67	0,00	0,13	66,17	0,00	0,07	0,19
43	52,56	0,36	0,02	66,10	0,06	0,02	0,19
44	52,48	0,43	-0,07	65,82	0,24	-0,28	0,35
45	52,13	0,49	-0,41	66,20	0,43	0,09	0,50
46	52,60	0,24	0,06	66,04	0,11	-0,06	0,12
47	51,82	0,33	-0,72	65,69	0,10	-0,41	1,13
48	52,58	0,34	0,03	65,91	0,14	-0,19	0,22
49	52,42	0,38	-0,13	65,72	0,14	-0,38	0,51
50	52,20	0,29	-0,35	65,88	0,17	-0,22	0,57
51	51,25	0,34	-1,29	65,28	0,11	-0,82	2,11
52	52,51	0,33	-0,03	65,76	0,29	-0,35	0,38
53	52,60	0,24	0,06	65,98	0,10	-0,13	0,19
54	52,67	0,41	0,13	66,01	0,11	-0,10	0,22
55	52,48	0,28	-0,06	65,91	0,14	-0,19	0,25
56	52,32	0,14	-0,22	65,72	0,06	-0,38	0,60
57	52,98	0,43	0,44	65,60	0,25	-0,50	0,94
58	52,95	0,10	0,41	65,98	0,00	-0,12	0,53
59	52,86	0,10	0,31	65,88	0,17	-0,22	0,53
60	52,86	0,10	0,31	65,76	0,14	-0,35	0,66
61	52,80	0,29	0,28	65,85	0,24	0,00	0,28
62	52,76	0,34	0,25	66,09	0,32	0,24	0,49
63	53,08	0,29	0,56	66,07	0,10	0,22	0,79
64	51,66	0,14	-0,85	65,60	0,09	-0,25	1,10
65	52,45	0,14	-0,07	65,95	0,14	0,10	0,16
66	52,57	0,10	0,06	65,91	0,07	0,06	0,12
67	51,82	0,48	-0,69	65,88	0,10	0,03	0,73
68	52,70	0,05	0,19	66,01	0,05	0,16	0,35
69	52,54	0,20	0,03	65,76	0,14	-0,09	0,12
70	52,92	0,11	0,41	66,42	0,14	0,57	0,98
71	52,57	0,20	0,06	65,79	0,10	-0,06	0,12
72	52,54	0,15	0,03	65,79	0,10	-0,06	0,09
73	50,40	0,10	-2,11	65,26	0,11	-0,59	2,70
74	51,03	0,11	-1,48	66,67	0,15	0,82	2,30
75	52,26	0,05	-0,25	65,88	0,10	0,03	0,29
76	52,83	0,14	0,31	65,88	0,10	0,03	0,35
77	52,57	0,17	0,06	65,79	0,25	-0,06	0,12
78	52,57	0,10	0,06	66,01	0,11	0,16	0,22
79	52,64	0,06	0,12	65,91	0,06	0,06	0,19
80	52,67	0,00	0,16	65,88	0,17	0,03	0,19
81	52,73	0,20	0,22	66,01	0,11	0,16	0,37
82	53,14	0,00	0,63	66,23	0,28	0,38	1,01
83	52,83	0,14	0,31	65,85	0,15	0,00	0,31
84	52,10	0,10	-0,41	66,42	0,38	0,57	0,98
85	52,95	0,28	0,44	66,48	0,20	0,63	1,07

86	52,80	0,22	0,28	66,04	0,31	0,19	0,47
87	53,02	0,06	0,50	66,04	0,45	0,19	0,69
88	52,92	0,27	0,40	66,23	0,20	0,38	0,78
89	52,70	0,20	0,19	66,20	0,28	0,35	0,54
90	52,71	0,41	0,34	65,73	0,29	0,00	0,34
91	52,59	0,14	0,22	66,20	0,00	0,47	0,69
92	52,65	0,05	0,28	66,26	0,15	0,53	0,82
93	52,43	0,09	0,06	65,69	0,11	-0,03	0,10
94	52,40	0,14	0,03	65,79	0,05	0,06	0,09
95	51,93	0,21	-0,44	65,88	0,14	0,16	0,60
96	52,49	0,05	0,12	66,32	0,07	0,60	0,72
97	52,40	0,05	0,03	65,82	0,09	0,09	0,13
98	52,24	0,17	-0,12	65,91	0,10	0,19	0,31
99	52,40	0,05	0,03	65,91	0,32	0,19	0,22
100	52,81	0,00	0,44	66,16	0,11	0,44	0,88
101	51,87	0,11	-0,50	65,88	0,19	0,16	0,66
102	52,52	0,16	0,16	65,82	0,09	0,09	0,25
103	52,68	0,28	0,31	66,13	0,33	0,41	0,72
104	52,52	0,16	0,16	66,20	0,41	0,47	0,63
105	52,46	0,10	0,09	65,91	0,19	0,19	0,28
106	52,40	0,05	0,03	66,10	0,19	0,37	0,41
107	48,60	0,30	-3,77	66,29	0,17	0,57	4,34
108	52,52	0,10	0,16	66,51	0,05	0,78	0,94
109	52,49	0,05	0,12	66,26	0,05	0,53	0,66
110	52,46	0,10	0,09	65,88	0,05	0,15	0,25
111	52,43	0,25	0,06	66,32	0,20	0,60	0,66
112	52,49	0,11	0,13	66,16	0,11	0,44	0,56
113	52,49	0,14	0,13	66,13	0,24	0,41	0,53
114	52,43	0,09	0,06	66,17	0,06	0,44	0,50
115	51,74	0,14	-0,63	66,10	0,10	0,38	1,01
116	52,81	0,00	0,44	66,45	0,20	0,72	1,17
117	52,40	0,20	0,03	66,54	0,36	0,82	0,85
118	52,71	0,34	0,35	66,32	0,14	0,60	0,94
119	52,52	0,10	0,16	66,54	0,05	0,81	0,97
120	52,57	0,17	0,10	66,04	0,15	0,28	0,38
121	52,48	0,17	0,00	66,20	0,20	0,44	0,44
122	52,60	0,14	0,13	66,07	0,10	0,32	0,44
123	50,84	0,19	-1,63	65,22	0,16	-0,53	2,17
124	48,54	0,45	-3,94	65,22	0,25	-0,53	4,47
125	52,48	0,10	0,00	65,92	0,11	0,16	0,16
126	52,64	0,14	0,16	66,39	0,39	0,64	0,80
127	51,19	0,11	-1,29	65,82	0,11	0,06	1,35
128	52,42	0,11	-0,06	65,82	0,05	0,06	0,12
129	52,42	0,24	-0,06	66,04	0,34	0,28	0,34
130	50,50	0,49	-1,98	63,87	0,43	-1,89	3,87

131	52,29	0,09	-0,19	65,57	0,14	-0,19	0,38
132	52,48	0,00	0,00	65,63	0,10	-0,13	0,13
133	52,51	0,11	0,03	66,04	0,20	0,28	0,31
134	52,70	0,22	0,22	66,35	0,41	0,60	0,82
135	52,35	0,05	-0,13	65,75	0,11	0,00	0,13
136	52,73	0,05	0,25	66,17	0,16	0,41	0,66
137	52,63	0,29	0,16	66,48	0,14	0,73	0,88
138	48,76	0,11	-3,71	66,83	0,00	1,07	4,79
139	52,54	0,15	0,06	65,85	0,22	0,10	0,16
140	52,29	0,00	-0,19	65,85	0,33	0,10	0,28
141	52,67	0,10	0,19	66,48	0,14	0,73	0,92
142	52,57	0,19	0,09	66,11	0,22	0,35	0,44
143	52,45	0,06	-0,03	65,76	0,06	0,00	0,03
144	52,79	0,36	0,32	66,32	0,24	0,57	0,88
145	52,54	0,05	0,06	66,26	0,17	0,51	0,57
146	52,20	0,10	-0,28	65,60	0,09	-0,16	0,44
147	50,25	0,11	-2,23	65,98	0,19	0,22	2,45
148	52,35	0,14	-0,12	65,98	0,35	0,22	0,34
149	48,13	0,02	-4,01	66,45	0,09	0,60	4,61
150	51,54	0,32	-0,60	66,14	0,06	0,29	0,89
151	52,22	0,46	0,09	66,45	0,34	0,60	0,68
152	51,94	0,20	-0,19	65,66	0,19	-0,19	0,38
153	51,79	0,36	-0,35	65,79	0,10	-0,06	0,41
154	52,10	0,00	-0,04	65,85	0,05	0,00	0,04
155	52,14	0,11	0,00	66,18	0,10	0,33	0,33
156	52,24	0,05	0,10	65,92	0,11	0,07	0,17
157	52,20	0,00	0,06	65,82	0,05	-0,03	0,09

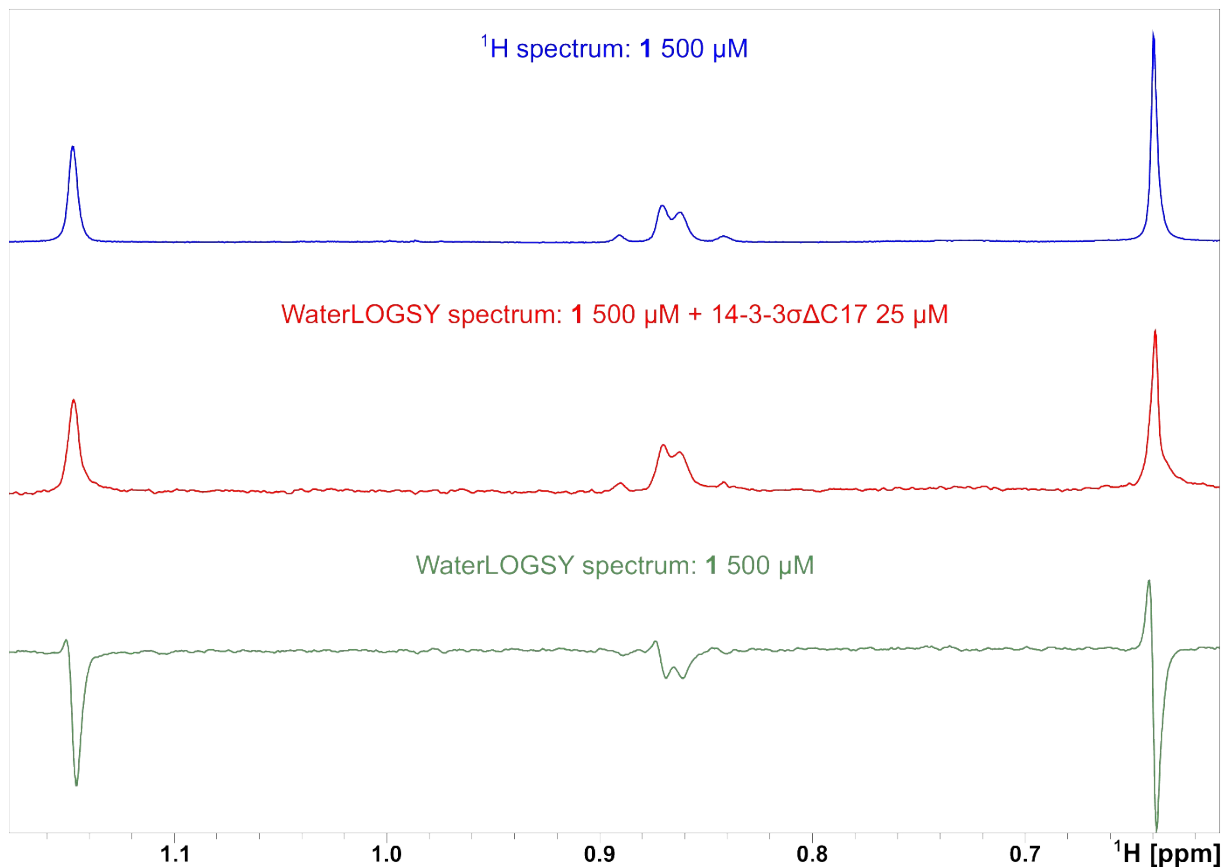


Figure S5. WaterLOGSY detects the binding of **1** to 14-3-3 $\sigma\Delta\text{C17}$. ^1H spectrum of **1** 500 μM (blue spectrum, on top). The WaterLOGSY spectrum of a solution containing **1** 500 μM and 14-3-3 $\sigma\Delta\text{C17}$ 25 μM (in red) shows that the NMR signals of **1** are phased positive, indicating binding. The control WaterLOGSY spectrum of a solution containing **1** 500 μM alone (in green) shows that in the absence of 14-3-3 $\sigma\Delta\text{C17}$ the NMR signals of **1** 500 μM are all phased negative.

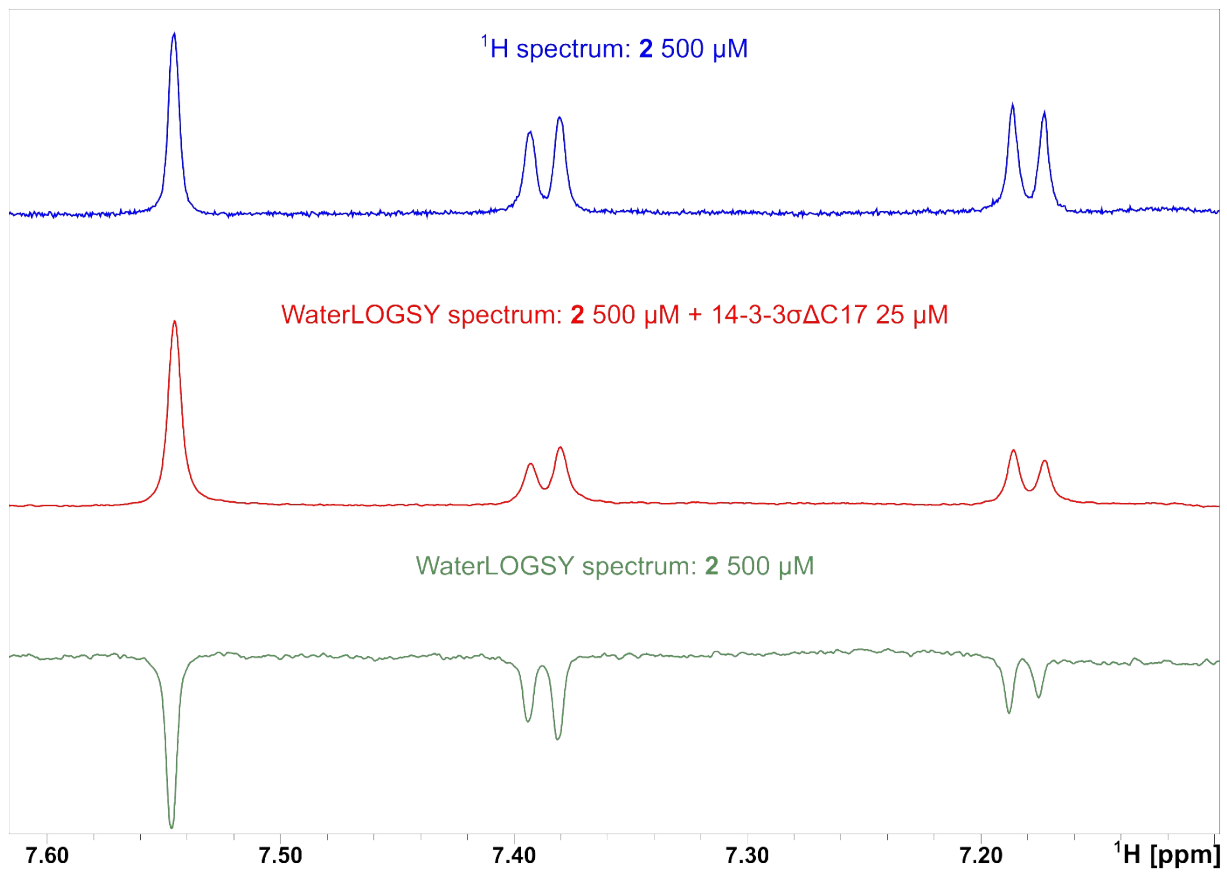


Figure S6. WaterLOGSY detects the binding of **2** to 14-3-3 σ ΔC17. ¹H spectrum of **2** 500 μM (blue spectrum, on top). The WaterLOGSY spectrum of a solution containing **2** 500 μM and 14-3-3 σ ΔC17 25 μM (in red) shows that the NMR signals of **2** are phased positive, indicating binding. The control WaterLOGSY spectrum of a solution containing **2** 500 μM alone (in green) shows that in the absence of 14-3-3 σ ΔC17 the NMR signals of **2** 500 μM are all phased negative.

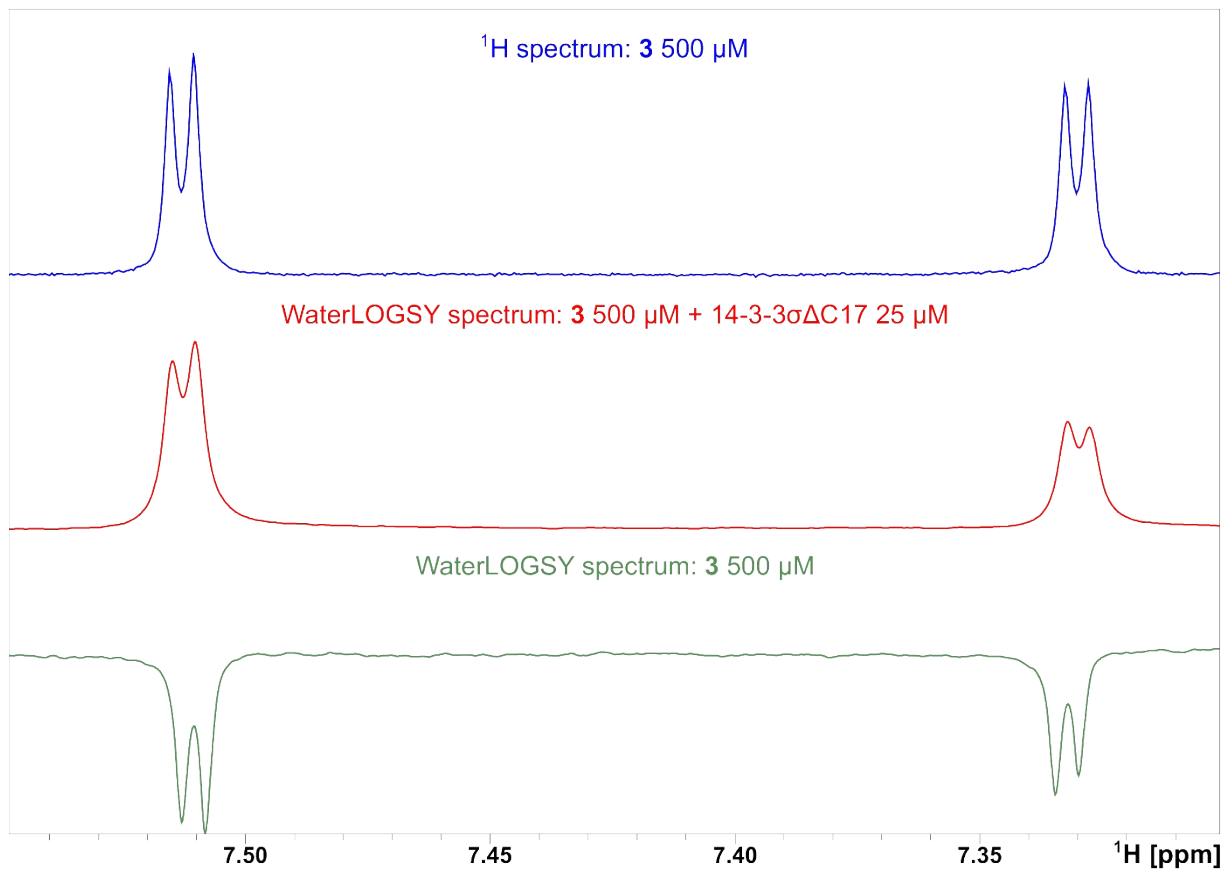


Figure S7. WaterLOGSY detects the binding of **3** to 14-3-3 $\sigma\Delta\text{C17}$. ¹H spectrum of **3** 500 μM (blue spectrum, on top). The WaterLOGSY spectrum of a solution containing **3** 500 μM and 14-3-3 $\sigma\Delta\text{C17}$ 25 μM (in red) shows that the NMR signals of **3** are phased positive, indicating binding. The control WaterLOGSY spectrum of a solution containing **3** 500 μM alone (in green) shows that in the absence of 14-3-3 $\sigma\Delta\text{C17}$ the NMR signals of **3** 500 μM are all phased negative.

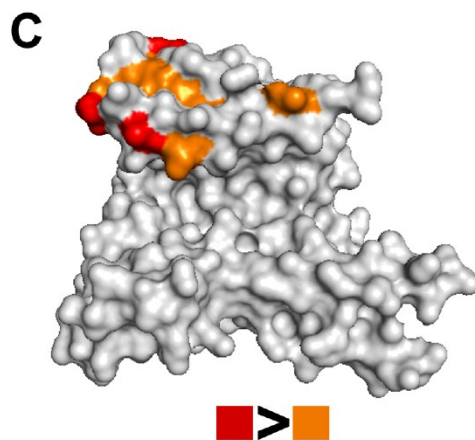
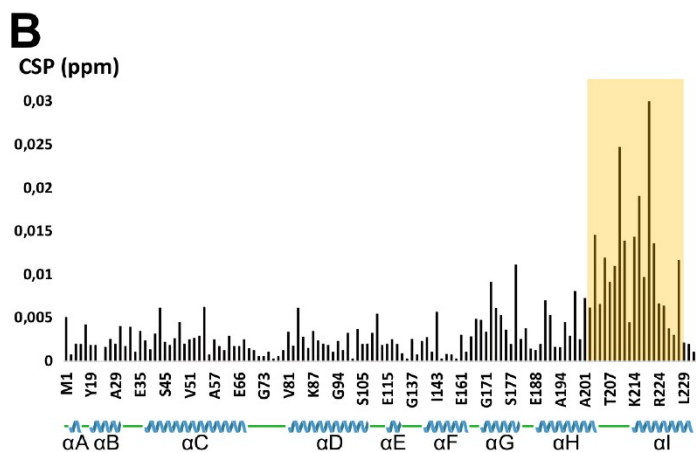
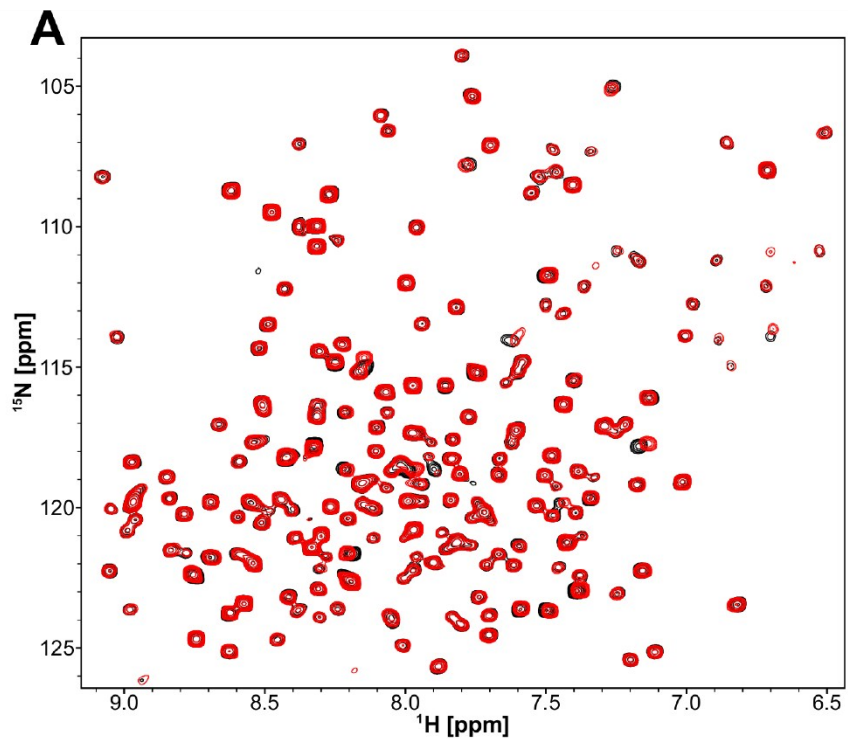


Figure S8. 1 binding site on 14-3-3 σ ΔC17 identified by ^1H - ^{15}N TROSY-HSQC. (A) Superimposed ^1H - ^{15}N TROSY-HSQC spectra of $^{15}\text{N}^2\text{H}$ labelled 14-3-3 σ ΔC17 75 μM in the presence of 2% DMSO-d₆ (v/v) (in black) and **1** 2000 μM (in red). (B) Plot of the CSP values (in ppm) of ^1H - ^{15}N correlation peaks of 75 μM 14-3-3 σ ΔC17 in the presence of 2000 μM **1** compared to the reference 14-3-3 σ ΔC17 spectrum (75 μM) (*y* axis) versus the amino acid sequence (*x* axis). A total of 128 correlation peak CSP are shown. The *x* axis is not proportional. The helices of 14-3-3 σ are identified below the *x* axis as blue cartoons, while disordered regions are represented by green lines. The area highlighted in yellow shows the region of the protein affected by the presence of **1**. (C) Mapping on the crystal structure of 14-3-3 σ (PDB ID: 1YZ5) of the amino acid residues corresponding to the 10 most affected resonances by the presence of **1**. The residues corresponding to the 5 most affected resonances are colored in red and an additional 5 are colored in orange.

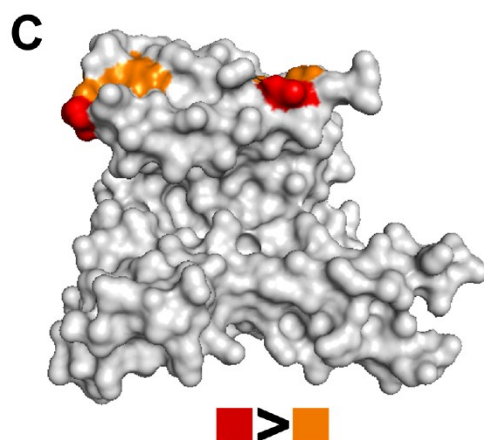
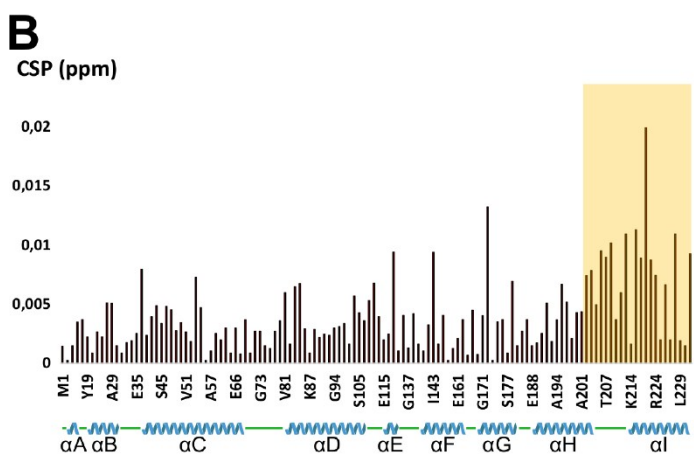
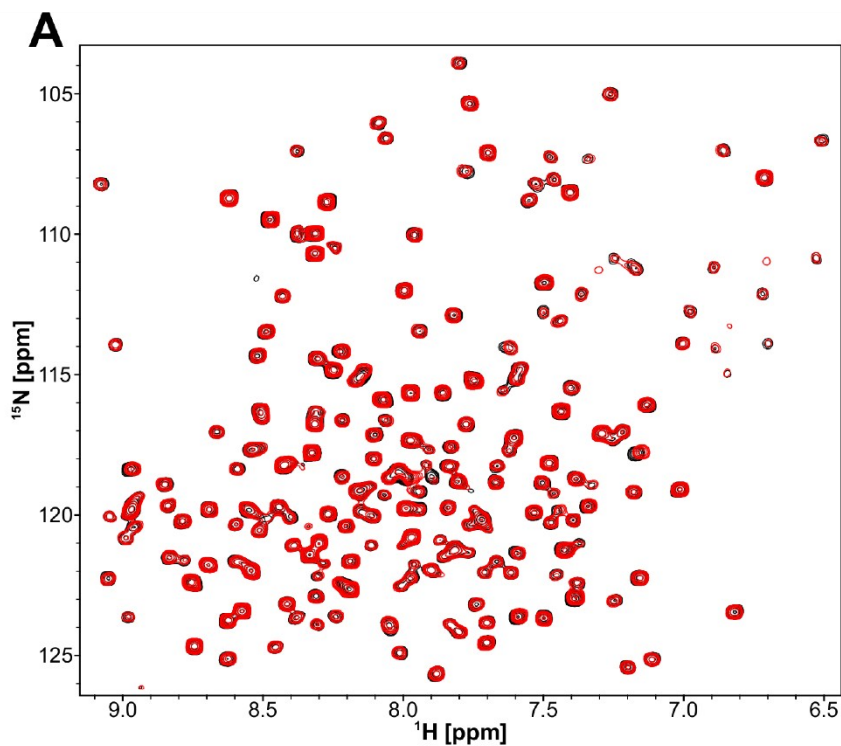


Figure S9. 2 binding site on 14-3-3 σ ΔC17 identified by ^1H - ^{15}N TROSY-HSQC. (A) Superimposed ^1H - ^{15}N TROSY-HSQC spectra of $^{15}\text{N}^2\text{H}$ labelled 14-3-3 σ ΔC17 75 μM in the presence of 2% DMSO-d₆ (v/v) (in black) and **2** 2000 μM (in red). (B) Plot of the CSP values (in ppm) of ^1H - ^{15}N correlation peaks of 75 μM 14-3-3 σ ΔC17 in the presence of 2000 μM **2** compared to the reference 14-3-3 σ ΔC17 spectrum (75 μM) (y axis) versus the amino acid sequence (x axis). A total of 128 correlation peak CSP are shown. The x axis is not proportional. The helices of 14-3-3 σ are identified below the x axis as blue cartoons, while disordered regions are represented by green lines. The area highlighted in yellow shows the region of the protein affected by the presence of **2**. (C) Mapping on the crystal structure of 14-3-3 σ (PDB ID: 1YZ5) of the amino acid residues corresponding to the 10 most affected resonances by the presence of **2**. The residues corresponding to the 5 most affected resonances are colored in red and an additional 5 are colored in orange.

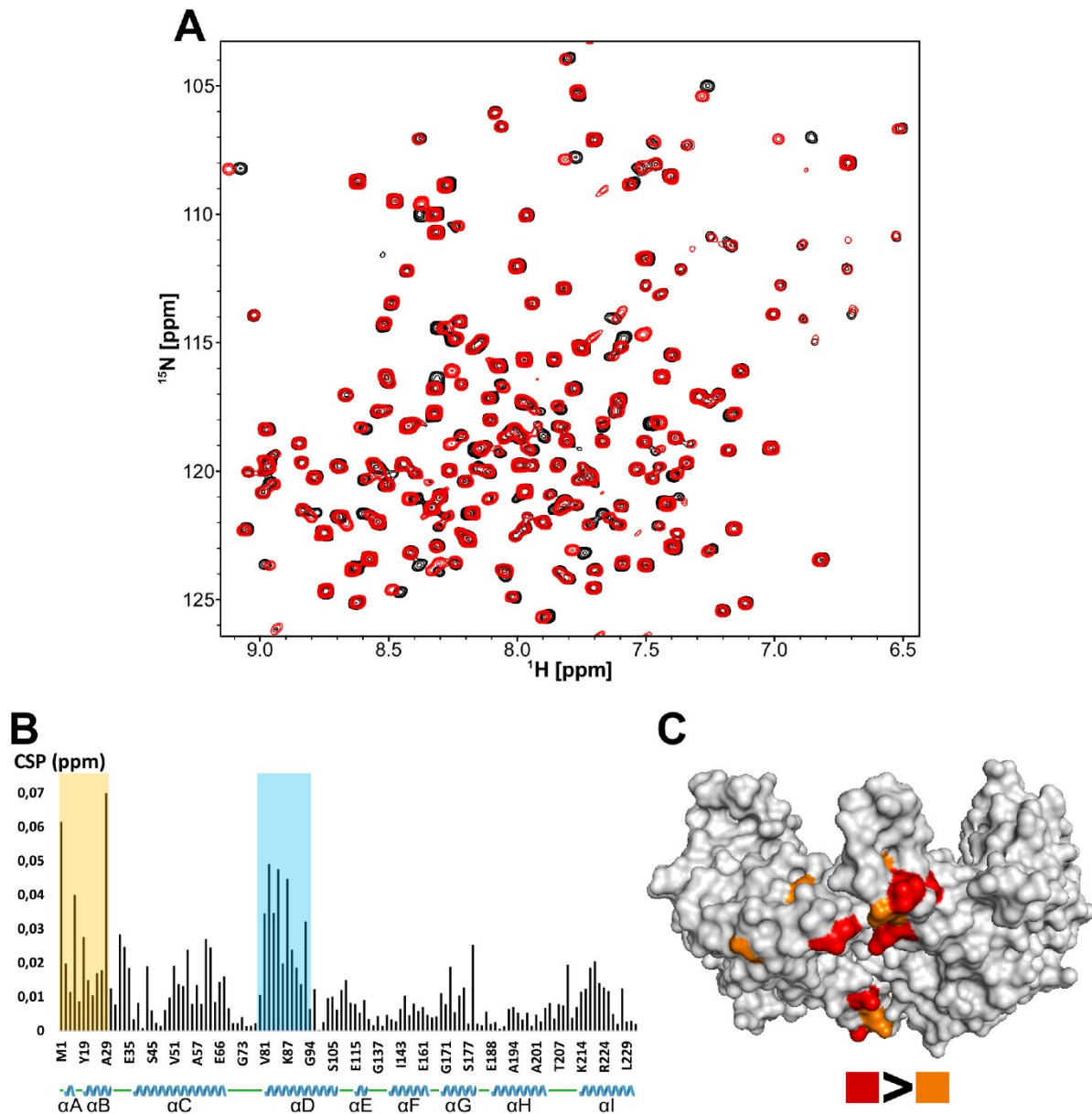


Figure S10. 3 binding site on 14-3-3 σ ΔC17 identified by ^1H - ^{15}N TROSY-HSQC. (A) Superimposed ^1H - ^{15}N TROSY-HSQC spectra of $^{15}\text{N}^2\text{H}$ labelled 14-3-3 σ ΔC17 75 μM in the presence of 2% DMSO- d_6 (v/v) (in black) and **3** 2000 μM (in red). (B) Plot of the CSP values (in ppm) of ^1H - ^{15}N correlation peaks of 75 μM 14-3-3 σ ΔC17 in the presence of 2000 μM **3** compared to the reference 14-3-3 σ ΔC17 spectrum (75 μM) (y axis) versus the amino acid sequence (x axis). A total of 128 correlation peak CSP are shown. The x axis is not proportional. The helices of 14-3-3 σ are identified below the x axis as blue cartoons, while disordered regions are represented by green lines. The areas highlighted in yellow and blue show the region of the protein affected by the presence of **3**. (C) Mapping on the crystal structure of 14-3-3 σ (PDB ID: 1YZ5) of the amino acid residues corresponding to the 10 most affected resonances by the presence of **3**. The residues corresponding to the 5 most affected resonances are colored in red and an additional 5 are colored in orange.